

Influence of surface nudging on climatological mean and ENSO feedbacks in a coupled model

Jieshun Zhu^{1,2} · Arun Kumar¹

Received: 9 August 2016 / Accepted: 8 March 2017 / Published online: 3 April 2017
© Springer-Verlag Berlin Heidelberg 2017

Abstract Studies have suggested that surface nudging could be an efficient way to reconstruct the subsurface ocean variability, and thus a useful method for initializing climate predictions (e.g., seasonal and decadal predictions). Surface nudging is also the basis for climate models with flux adjustments. In this study, however, some negative aspects of surface nudging on climate simulations in a coupled model are identified. Specifically, a low-resolution version of the NCEP Climate Forecast System, version 2 (CFSv2L) is used to examine the influence of nudging on simulations of climatological mean and on the coupled feedbacks during ENSO. The effect on ENSO feedbacks is diagnosed following a heat budget analysis of mixed layer temperature anomalies. Diagnostics of the climatological mean state indicates that, even though SST biases in all ocean basins, as expected, are eliminated, the fidelity of climatological precipitation, surface winds and subsurface temperature (or the thermocline depth) could be highly ocean basin dependent. This is exemplified by improvements in the climatology of these variables in the tropical Atlantic, but degradations in the tropical Pacific. Furthermore, surface nudging also distorts the dynamical feedbacks during ENSO. For example, while the thermocline feedback played a critical role during the evolution of ENSO in a free simulation, it only played a minor role in the nudged simulation. These results imply that, even though the simulation of surface temperature could

be improved in a climate model with surface nudging, the physics behind might be unrealistic.

1 Introduction

In its simplest conceptual form, the thermodynamic equation governing the sea surface temperature (SST) can be written as:

$$\frac{\partial T}{\partial t} = Q_0 + Q_D, \quad (1)$$

which describes the tendency of SST to be determined by two processes: the net local air-sea heat exchanges (Q_0) including the solar and longwave radiation, sensible and latent heat flux, and the oceanic heat transports (Q_D) consisting of horizontal and vertical temperature advections, entrainment of cold water into the oceanic mixed layer, sub-scale temperature diffusion and the penetrating solar radiation through the bottom of the mixed layer. In the coupled model simulations with surface nudging, Eq. (1) gets modified as follows:

$$\frac{\partial \tilde{T}}{\partial t} = \tilde{Q}_0 + \tilde{Q}_D + \Delta Q, \quad (2)$$

where ΔQ represents the additional nudging (restoring) effect.

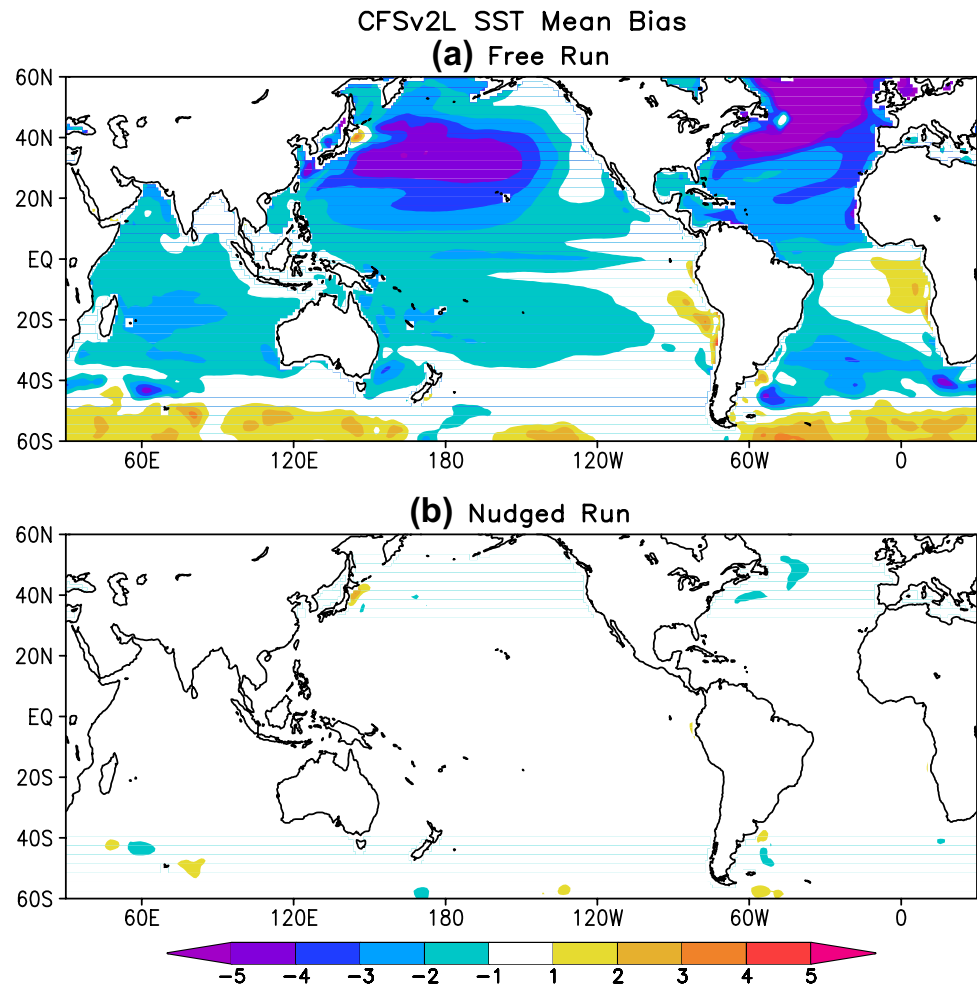
Studies have suggested that surface nudging could be an efficient way to reproduce the subsurface thermal variability (e.g., Kumar et al. 2014a, b; Servonnat et al. 2015; Ray et al. 2015). For example, Kumar et al. (2014a, b) demonstrated that coupled model integration with SST continuously nudged to the observed state can generate a realistic evolution of subsurface ocean temperatures; the evolution of slow variability related to ENSO, in particular, has a

✉ Jieshun Zhu
jieshun.zhu@noaa.gov

¹ Climate Prediction Center, NOAA/NWS/NCEP, 5830 University Research Court, College Park, MD 20740, USA

² Earth System Science Interdisciplinary Center, University of Maryland, College Park, MD, USA

Fig. 1 Climatological mean SST bias (°C) relative to OISST SST in **a** the Free Run, **b** the Nudged Run



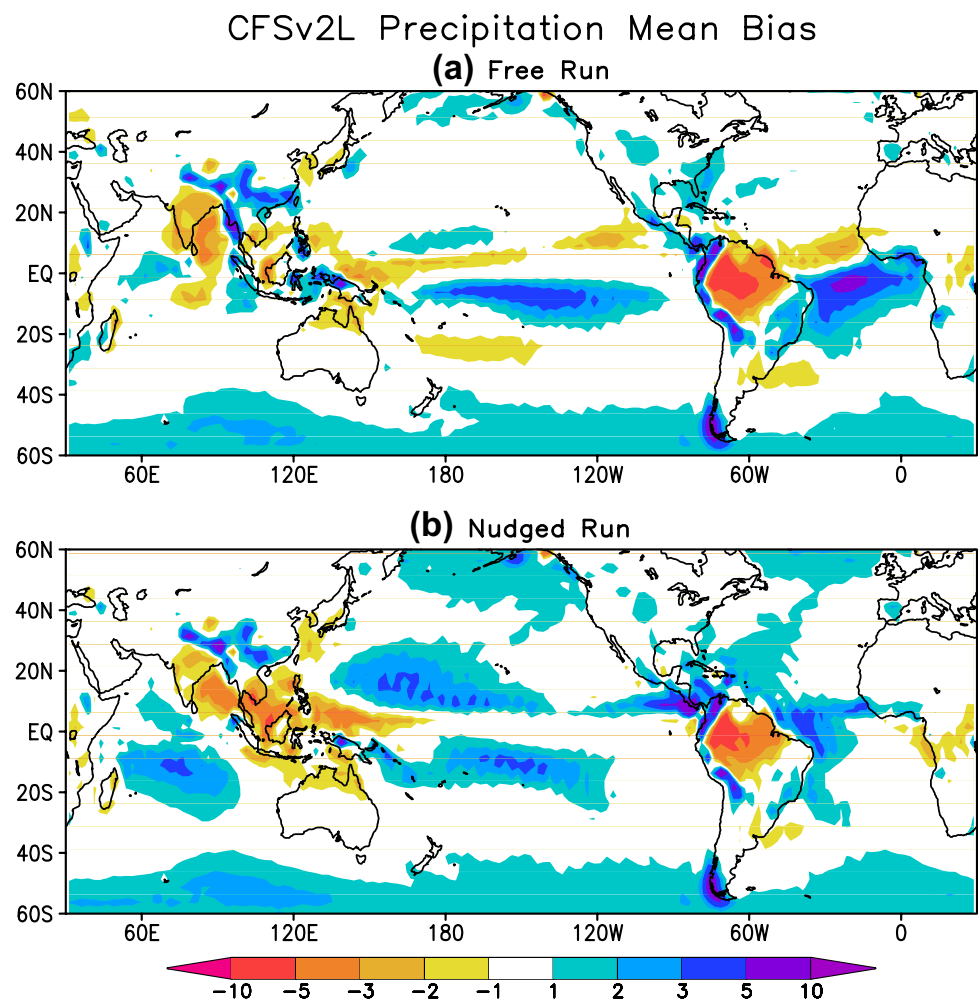
good resemblance to its observational counterpart. Further, Servonnat et al. (2015), in a perfect model framework, found that while nudging SST is enough to reconstruct the subsurface thermal condition in the tropics, sea surface salinity (SSS) nudging is also required in the mid-to-high latitudes. The physical basis for the success of nudging approach in simulating realistic sub-surface ocean variability is that, in addition to providing a realistic oceanic mixed layer temperature because of nudging, the observed SST information, through air-sea interaction and coupling adds further to the simulation of sub-surface variability via its ability to also partially reproduce observed surface winds (Kumar et al. 2014a, b).

The surface nudging, therefore, could be a useful initialization scheme for climate predictions from seasonal (e.g., Keenlyside et al. 2005; Luo et al. 2005, 2007; Zhu et al. 2015a, 2017a) to decadal (e.g., Keenlyside et al. 2008; Swingedouw et al. 2013) time scales, because the climate predictability mainly resides in the sub-surface ocean memory. Indeed, evidence for skillful predictions has been presented based on the simple initialization schemes. For instance, most recently Zhu et al. (2017a) found that

for predictions of SST, 2-m temperature and precipitation over land, prediction skill by the simple ocean initialization procedure was well within the range of skills of predictions that were initialized by the sophisticated data assimilation schemes. This result suggested that most present-day capabilities of seasonal predictions can be captured by utilizing a simpler SST only initialization procedure. In comparison with the sophisticated initialization scheme that assimilates subsurface ocean observations as well, even if surface nudging might have somewhat less potential to realize climate predictability, it can be used to extend climate hindcasts farther back because of the availability of longer SST records than of subsurface ocean observations. The advantage is especially valuable for studies of decadal predictions and predictability (e.g., Meehl et al. 2014), for which initialization using sophisticated initialization schemes can hardly produce enough independent forecast samples.

In addition, surface nudging is also the basis for climate models with flux adjustments. The adjustment term in the flux-corrected models is usually estimated based on prior runs where fluxes [i.e., ΔQ in Eq. (2)] necessary to maintain simulated temperatures close to the

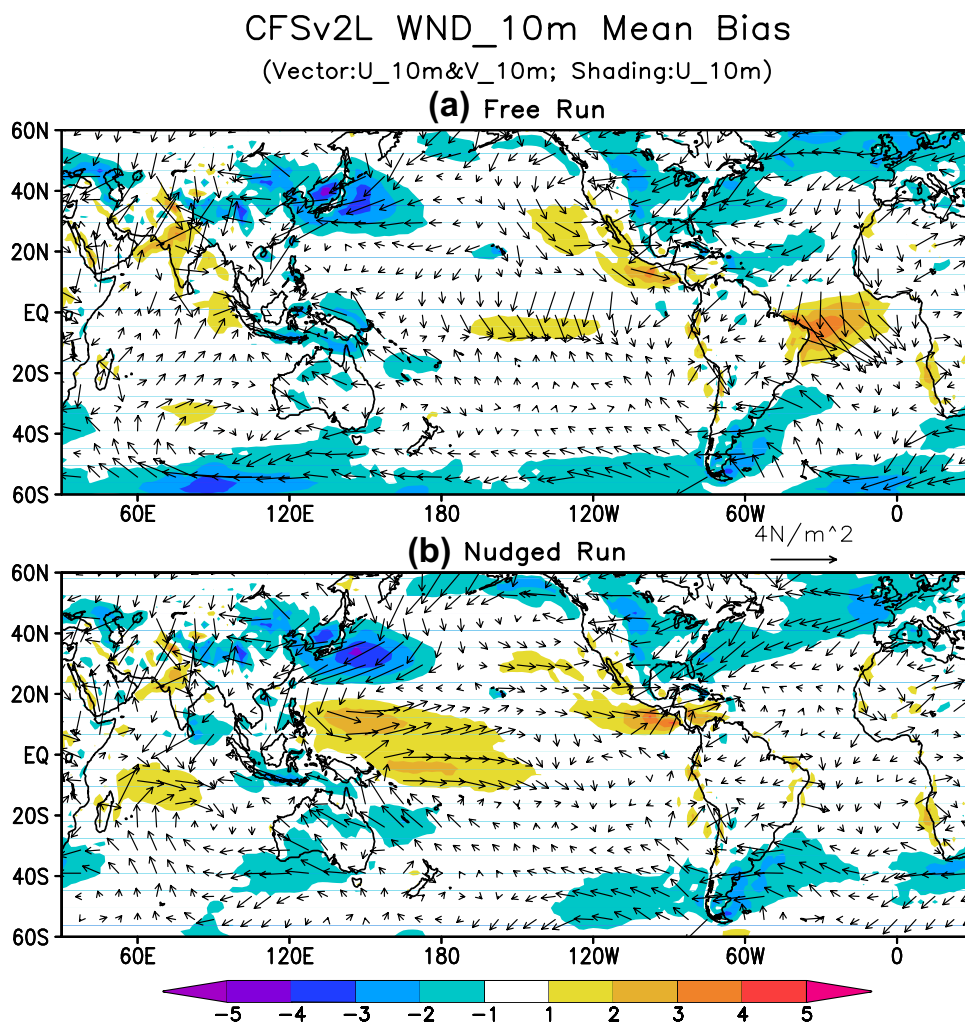
Fig. 2 Same as in Fig. 1, but for precipitation relative to CMAP precipitation



observed climatology are first estimated. Taking the procedure by Xiang et al. (2012) as an example, monthly ΔQ from a strong SST restoring simulation was saved, and its long-term mean was then added to the SST equation of the model, thereby constructing a flux-corrected version of the model. By including the adjustment term, the flux-corrected model tries to mimic the properties of the nudged run. However, there are differences between nudged and flux-corrected experiments. For example, the flux-corrected simulation generates its own ENSO variability, while the nudged simulation is restored to a specified ENSO variability (e.g., the observed one). Even though the strategy of flux adjustments fell out of favor of the scientific community for a while, it has seen a comeback in recent years (e.g., Spencer et al. 2007; Manganello and Huang 2009; Pan et al. 2011; Kröger and Kucharski 2011; Xiang et al. 2012; Magnusson et al. 2013a, b; Vecchi et al. 2014), mainly for the pragmatic purpose of improving the skill of dynamical climate predictions and projections which are thought to be negatively influenced by biases in SSTs.

Given the utility of the surface nudging method, further investigations with diverse climate models are required to understand the physical processes related to it, e.g., how the physical mechanisms associated with the ENSO could be affected by it. In this study, such an analysis is conducted with a low-resolution version of the NCEP Climate Forecast System, version 2 (CFSv2L), and two questions are addressed: (a) how are the climatological mean states of some key variables other than SST affected? (b) Are ENSO-related feedbacks modified by the surface nudging in coupled models? Previous studies about nudged simulations were mostly focused on the assessment about how well the observed variability (especially the subsurface thermal condition) was reproduced (e.g., Kumar et al. 2014a, b; Servonnat et al. 2015; Ray et al. 2015), but few assessed how physics behind the variability are modified by the nudging. In fact, when the nudged term [i.e., ΔQ in Eq. (2)] is included in a model, the other terms (i.e., Q_D) are also expected to change. For example, in a coupled model used by Xiang et al. (2012), the thermocline feedback during ENSO is enhanced by correcting the mean SST bias

Fig. 3 Same as in Fig. 1, but for 10-m winds relative to CFSR winds. Vectors (colors) are for wind vectors (zonal winds; m/s)



with a flux adjustment. However, as will be illustrated, there is also a possibility that the representation of climatological states and coupled feedbacks could be degraded by the surface nudging.

The paper is arranged as follows. The model, experiments, datasets and diagnostic methods are described in the next section. Results are presented in Sect. 3 that include the influence of nudging on the simulation of climatological mean state and on the characteristics of coupled feedbacks during ENSO. The summary and discussion are given in Sect. 4.

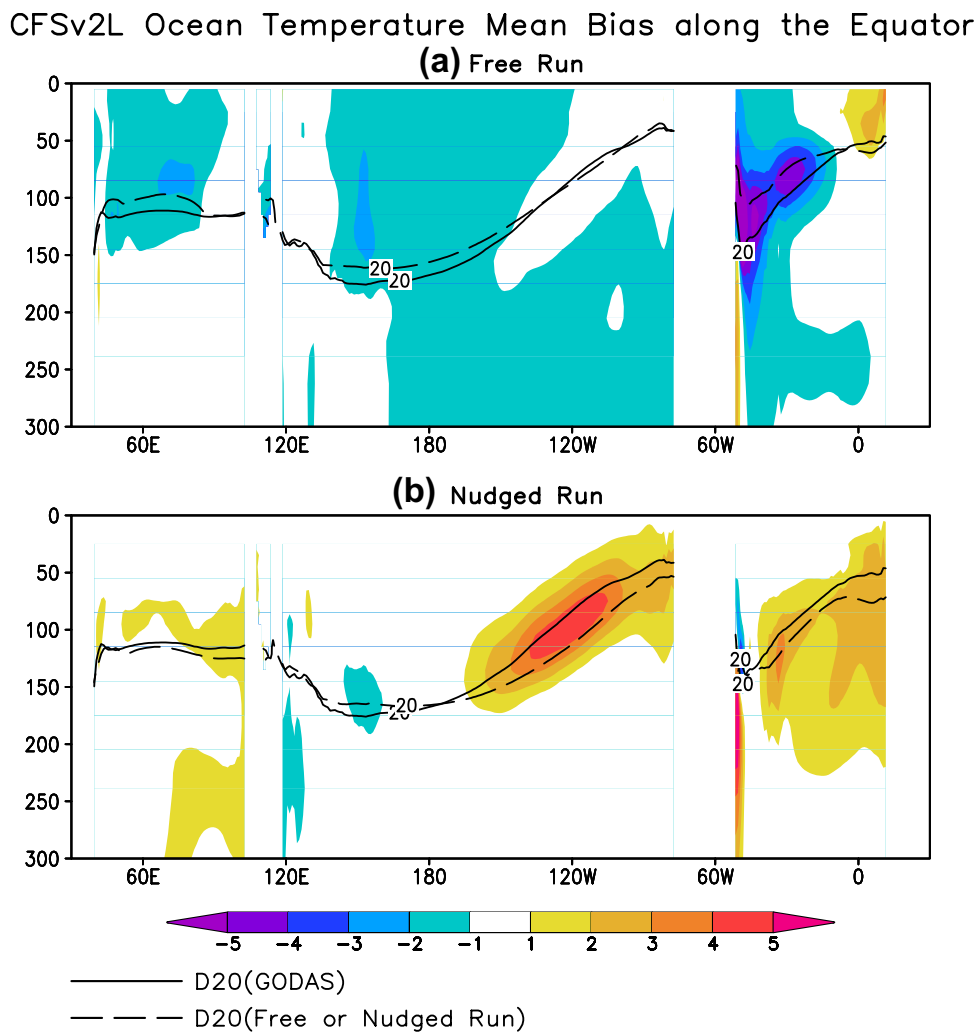
2 Model, experiments and datasets

The model used in this study is a variant of NCEP CFSv2 (Saha et al. 2014) with lower horizontal resolutions in both atmospheric and oceanic components. A lower resolution is simply to enhance throughput. To distinguish from the standard CFSv2 currently used for the operational seasonal-to-interannual prediction at NCEP, the low-resolution

CFSv2 is referred to as CFSv2L. In CFSv2L, the ocean model is the GFDL MOM version 4, which is configured for the global ocean with a horizontal grid of $1^\circ \times 1^\circ$ poleward of 30°S and 30°N and meridional resolution increasing gradually to 0.33° between 10°S and 10°N . The vertical coordinate is geopotential (z -) with 40 levels (27 of them in the upper 400 m), with maximum depth of approximately 4.5 km. The atmospheric model of CFSv2L is the Global Forecast System, which has horizontal resolution at T62, and 64 vertical levels in a hybrid sigma-pressure coordinate. The oceanic and atmospheric components of CFSv2L exchange surface momentum, heat and freshwater fluxes, as well as SSTs, every 60 min. CFSv2L has been used for studies about seasonal predictability (Zhu et al. 2017a) and MJO (Zhu et al. 2017b).

In this study, two experiments based on CFSv2L are compared to explore the impact of surface restoring on climate simulations. The first one (referred to as the Free Run) is initialized from the Climate Forecast System Reanalysis (CFSR; Saha et al. 2010) state on 1 January 1980, and run for 40 years. The outputs for the last 30 years are used for

Fig. 4 Climatological mean temperature bias (°C) along the equator relative to GODAS temperature for **a** the Nudged Run, **b** the Free Run. The solid (dashed) contour is the 20°C isotherms in GODAS (the Free or Nudged Run)



analyses. The second simulation (referred to as the Nudged Run) is where the model SST is nudged to the observed daily SST. The restoring time scale for the nudging is chosen as 3.3 days, a time scale following previous work with CFSv1 (Wang et al. 2013; Kumar et al. 2014a, b). The observed daily SSTs are interpolated from the monthly SSTs from the National Oceanic and Atmospheric Administration (NOAA) Optimum Interpolation SST (OISST) version 2 (Reynolds et al. 2002). Some initial analysis of the Nudged Run suggests that the evolution of subsurface ocean temperature were more realistically achieved by CFSv2L than by CFSv1 (Zhu et al. 2017a). Also, starting from the initial states from the Nudged Run, promising seasonal prediction skill was achieved (Zhu et al. 2017a). In this study, the Nudged Run is evaluated for its simulations during 1984–2013.

The datasets applied for comparison include monthly SST from OISST (Reynolds et al. 2002), monthly precipitation from the National Oceanic and Atmospheric Administration’s (NOAA) Climate Prediction Center Merged

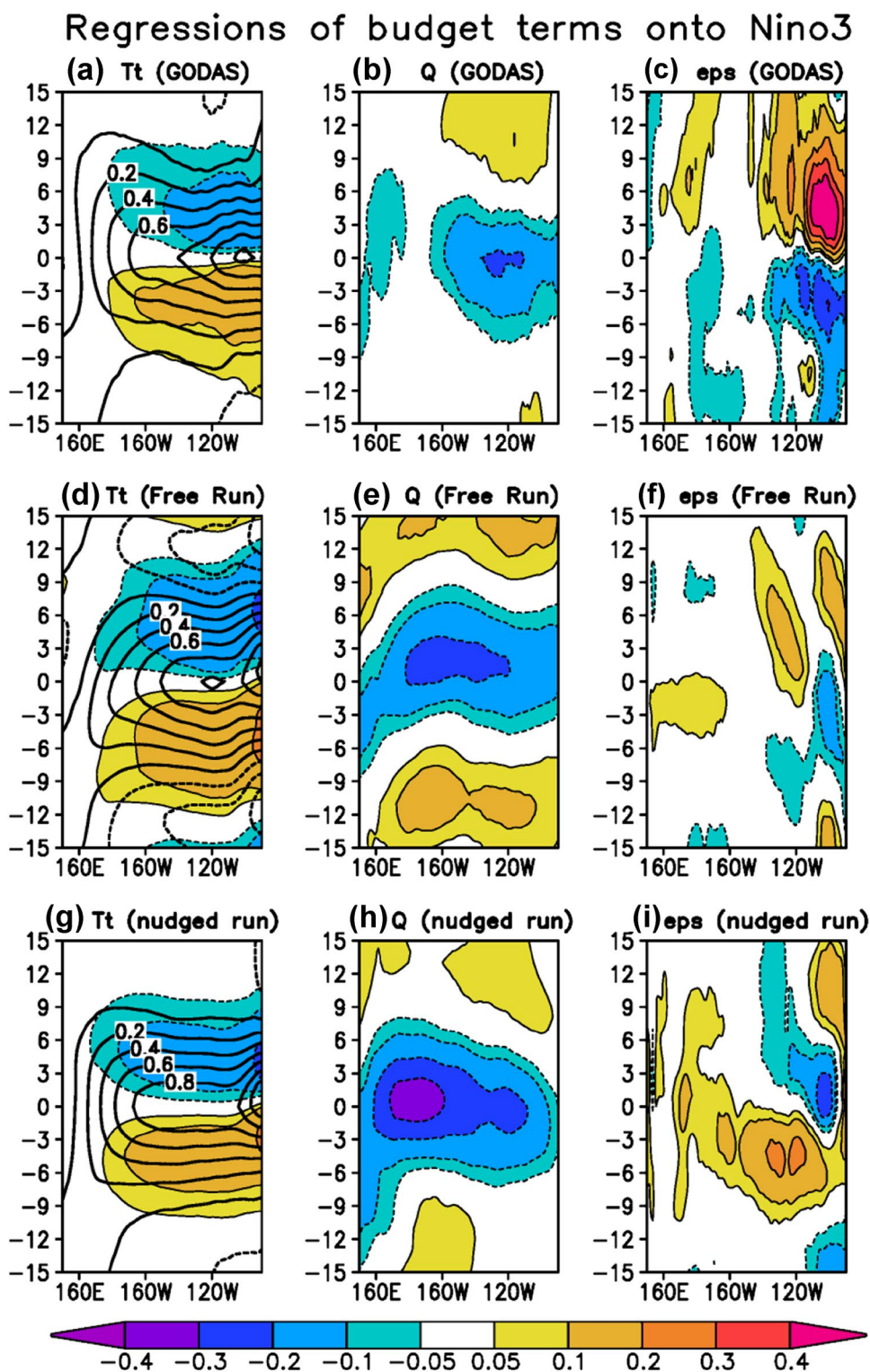
Analysis of Precipitation (CMAP) (Xie and Arkin 1997), monthly wind fields from CFSR (Saha et al. 2010), and monthly subsurface ocean temperatures from the NCEP Global Ocean Data Assimilation System (GODAS; Behringer and Xue 2004). Their climatological mean states are calculated based on 1984–2013.

3 Results

3.1 Impact on climatological mean

In this section, we explore the influence of surface nudging on the simulated climatological mean states. Figure 1 presents the global SST mean biases relative to the OISST climatology in the Free Run and the Nudged Run. As expected, the Nudged Run shows negligible SST biases. In the Free Run, the global SSTs in CFSv2L are generally too cold, except some warm biases in the southeastern tropical Pacific and Atlantic Oceans, and the Southern Ocean. The

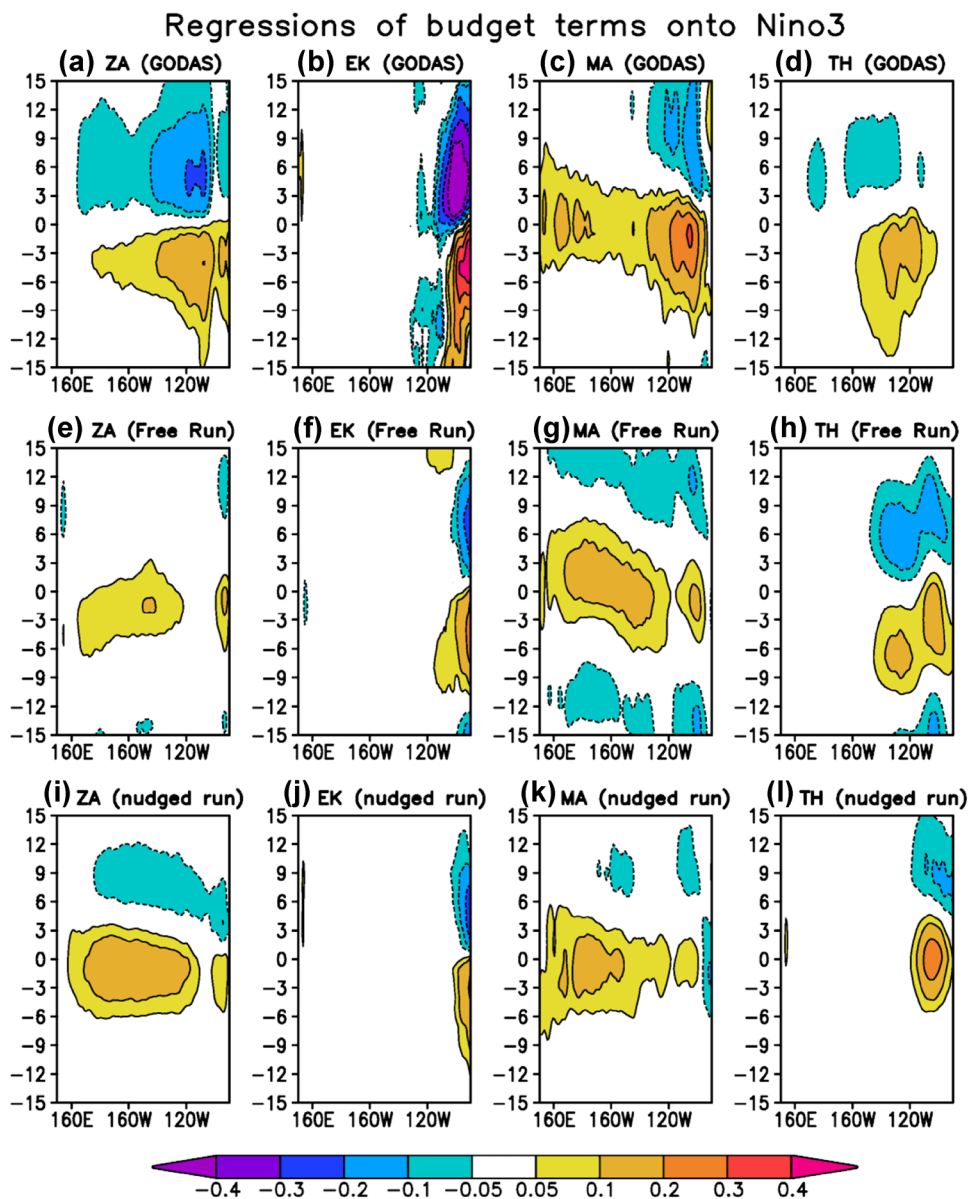
Fig. 5 Longitude-time lag section of terms in Eq. (3) regressed onto Niño-3 index in a–c GODAS, d–f the Free Run and g–i the Nudged Run: a, d, g T_t (the tendency of temperature anomalies), b, e, h Q (the net heat flux term) and c, f, i eps (the residual term). Units are month^{-1} . Black contours in a, d, g represents the regressions of mixed layer temperature against Niño-3 index. All regressions are shown along the equator averaged between 5°S and 5°N



cold bias is especially evident in the extratropical Pacific and the North Atlantic where the bias reaches below -5°C , while it is lower in the tropical ocean, generally less than -2°C . Specifically, the tropical Indian Ocean is featured by a uniform cold bias. Over the tropical Pacific, in addition to

the cold bias, there is also a slight warm bias in the south-eastern tropical Pacific Ocean. Over the tropical Atlantic, the SST bias is featured by a meridional pattern with the North (South) tropical Atlantic exhibiting a cold (warm) bias.

Fig. 6 Same as in Fig. 5, but for **a, e, i** the zonal advective feedback term (ZA), **b, f, j** the Ekman pumping feedback term (EK), **c, g, k** the mean current effect term (MA) and **d, h, l** the thermocline feedback term (TH)



The spatial pattern of differences in climatological mean precipitation (Fig. 2), to some extent are consistent with the differences in SSTs in that warmer SSTs in the nudged runs (compared to the free run) are generally associated with higher mean precipitation. However, although by construction SSTs in the nudged runs are closer to the observed everywhere, it is not the case for precipitation, i.e., an increase in precipitation bias also occurs over some basins. For example, in the tropical Indian Ocean while there is no well-organized precipitation bias in the Free Run, there is a wet bias of 3 mm/day in the southwestern tropical Indian Ocean in the Nudging Run. Also, in the tropical Pacific, even though the wet bias seems slightly reduced in the Nudged Run over the South Pacific convergence zone (SPCZ) region, the precipitation biases are

clearly enhanced in the north, particularly over the tropical western North Pacific (TWNP) region where a wet bias is clearly seen. The TWNP precipitation bias in the Nudged Run might be caused by lack of coupling, which otherwise will play a damping role in the occurrence of convections as in the Free Run (Zhu and Shukla 2013). For the tropical Atlantic basin, while the precipitation bias in the Nudged Run might be caused by the same mechanism as over the TWNP, its counterpart in the Free Run seems to be related to the SST bias pattern, featured by the southward migration of the Intertropical convergence zone (ITCZ; Fig. 2a) which occurs as a response to the SST meridional pattern by the same mechanism as in the Atlantic Meridional Mode (AMM; e.g., Moura and Shukla 1981; Huang and Shukla 1997).

Regressions of budget terms onto Nino3

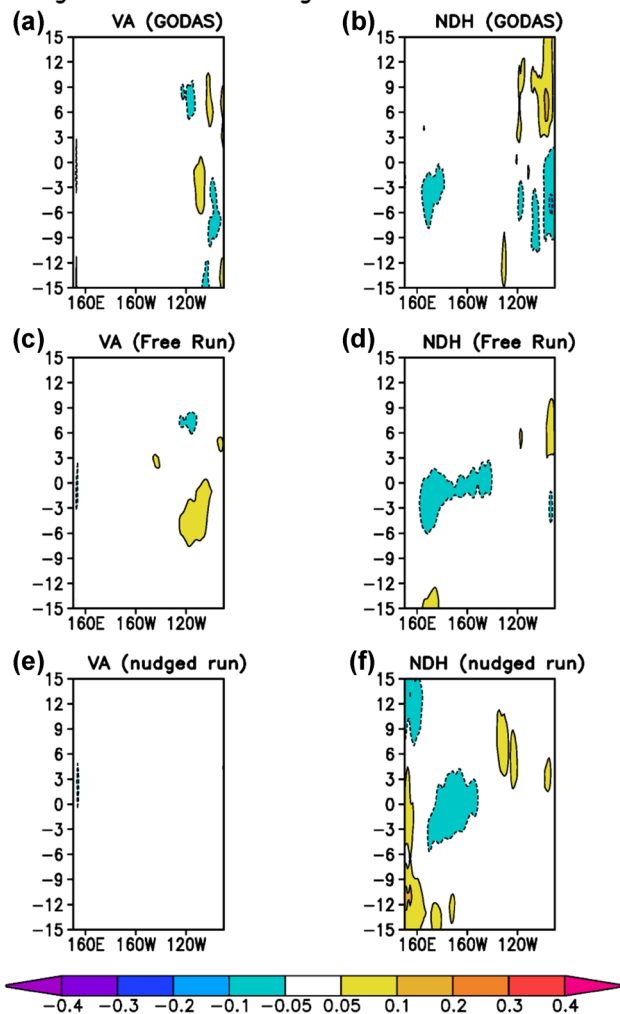


Fig. 7 Same as in Fig. 5, but for **a, c** the meridional advective effect term (VA) and the nonlinear dynamical heating term (NDH)

Associated with the precipitation biases, there are clear and physically consistent differences in surface winds and subsurface ocean thermal conditions. For the tropical Pacific, in contrast to Magnusson et al. (2013a) who demonstrated reduced wind biases because of surface nudging in a version of ECMWF coupled model (i.e., the ECMWF IFS model, version 36r1), in CFSv2L surface nudging clearly degrades the wind simulations (Fig. 3a vs. b). In particular, while only some marginal meridional wind biases are present in the central Pacific in the Free Run, significantly larger zonal wind biases (reaching 2 m/s) are present in the western Pacific in the Nudged Run, indicative of weakened trade winds over the tropical Pacific by surface nudging. As a consequence of the weakened trade winds, the subsurface thermal conditions are also significantly modulated, featured by a flattened thermocline along the equator in the Nudged Run (Fig. 4b). Correspondingly, in

the Free Run the thermocline depth is close to that in observations with negligible biases in subsurface temperature, but in the Nudged Run the thermocline is clearly deeper in the eastern Pacific (by ~ 20 m) with the ocean temperature along the thermocline 4°C higher than in observations and the Free Run (Fig. 4a vs. b). As will be seen in next section, the climatological bias in thermocline depth exerts a significant effect on dynamical feedbacks during ENSO (particularly the thermocline feedback) in the Nudged Run.

Over the tropical Indian Ocean, the surface winds are also influenced by surface nudging, from little wind biases in the Free Run (Fig. 3a) to noticeable westerly biases over the southwestern tropical Indian Ocean in the Nudged Run (Fig. 3b). The westerly biases in the Nudged Run are part of a local cyclonic wind bias (Fig. 3b), which corresponds to too much local precipitation in the Nudged Run (Fig. 2b). In terms of subsurface ocean, slightly shallower thermocline along the equator is simulated in the Free Run is changed to slightly deeper thermocline in the Nudged Run, and there are also consistent subsurface temperature changes.

Over the tropical Atlantic Ocean, SST nudging seems to improve the climatological simulations in both winds and subsurface conditions. In the Free Run, in correspondence to the AMM-type biases in SST and precipitation, strong cross-equatorial wind biases are evident, particularly over the western and central Atlantic. The meridional wind bias along the western coast would induce extra Ekman pumping, and thereby large cold biases (reaching -5°C) are present in the western basin (Fig. 4a). As a result of the cold biases together with westerly wind biases along the equator, the thermocline is too flat in the Free Run in comparison with GODAS. On the other hand, when surface nudging is applied in CFSv2L, the wind biases over the basin become much smaller (Fig. 3b), and consistently, the thermocline exhibits a structure similar to as in GODAS (Fig. 4b).

In summary, the above analyses suggest that the effect of surface nudging on simulating climatological mean states might depend on different basins. In CFSv2L, while nudging clearly improved the climatological simulations over the tropical Atlantic, it degraded the simulations over the tropical Pacific, and the effect on the tropical Indian Ocean was generally smaller than the two tropical basins.

3.2 Impact on coupled feedbacks during ENSO

Now, we examine how the coupled feedbacks during ENSO are sensitive to surface nudging. We focus on ENSO variability because its global impacts and its critical role in global climate predictions. For analyzing the coupled feedbacks, a heat budget analysis of mixed layer temperature anomalies is conducted. In this study, the mixed layer depth is roughly taken as the constant of 50 m for a qualitative

Regressions of budget terms onto Niño3 (Lag=-6 mon): GODAS

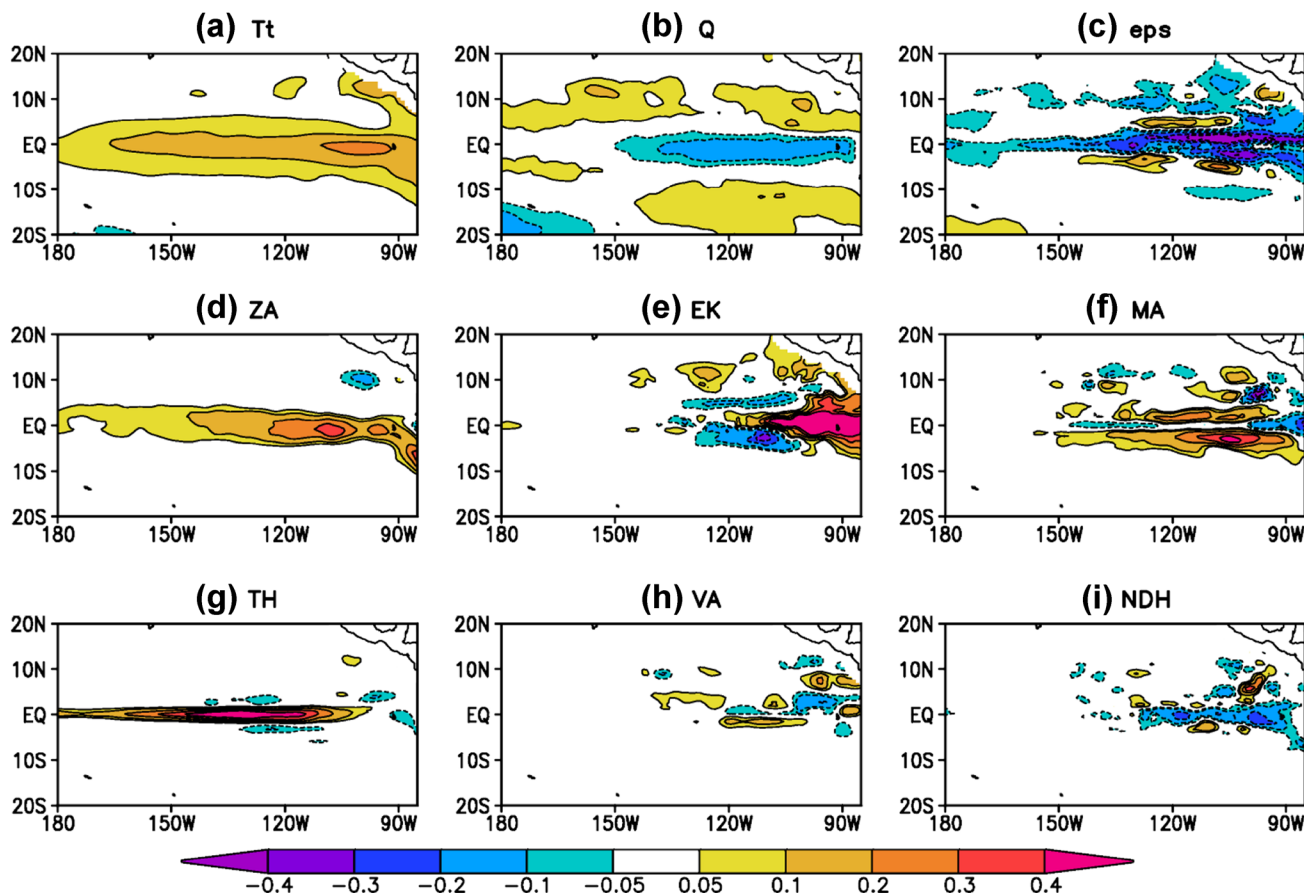


Fig. 8 Horizontal distribution of terms in Eq. (3) regressed onto Niño-3 index at the lag time of -6 months in GODAS (corresponding to 6 months before the peak phase of El Niño): **a** T_t (the tendency of temperature anomalies), **b** Q (the net heat flux term), **c** ϵ_{ps} (the residual term), **d** ZA (the zonal advective feedback term), **e** EK (the

Ekman pumping feedback term), **f** MA (the mean current effect term), **g** TH (the thermocline feedback term), **h** VA (the meridional advective effect term) and **i** NDH (the nonlinear dynamical heating term). Units are month^{-1}

exploration, an approach which has been used in many studies (e.g., Kang et al. 2001; Jin et al. 2003; An and Jin 2004). For the heat budget analysis, the following equation (e.g., Kang et al. 2001; Jin et al. 2003; Zhu et al. 2011) is applied:

approximates the mixed layer depth, and ϵ means the residual term (including the diffusive effects in two runs as well as the restoring effects in the Nudged Run). The vertical advection term is determined by the difference between the 50 m-averaging temperature and the temperature at the

$$\frac{\partial T'}{\partial t} = \underbrace{-u' \frac{\partial \bar{T}}{\partial x}}_{ZA} - \underbrace{v' \frac{\partial \bar{T}}{\partial y}}_{VA} - \underbrace{w' \frac{\partial \bar{T}}{\partial z}}_{EK} - \underbrace{-\bar{u} \frac{\partial T'}{\partial x} - \bar{v} \frac{\partial T'}{\partial y} - \bar{w} \frac{\partial T'}{\partial z}}_{MA} - \underbrace{-u' \frac{\partial T'}{\partial x} - v' \frac{\partial T'}{\partial y} - w' \frac{\partial T'}{\partial z}}_{TH} + \frac{Q'}{\rho C_p H} + \epsilon, \tag{3}$$

where $\bar{(\cdot)}$ means the climatological annual cycle, $(\cdot)'$ means monthly mean anomalies, $(\partial/\partial x, \partial/\partial y, \partial/\partial z)$ denotes the 3D gradient operator, T represents the mean temperature in the uppermost 50 m, (u, v, w) denotes the 3-dimensional ocean current, Q stands for the net heat flux into the ocean, $\rho = 1022.4 \text{ kg/m}^3$ is the density of seawater, $C_p = 3940 \text{ J/kg}^\circ\text{C}$ is the heat capacity of sea water, $H = 50 \text{ m}$

65 m depth.

In Eq. (3), except for tendency (T_t), net heat flux (Q) and residual (ϵ), the remaining terms could be categorized into six feedback processes, i.e., the zonal advective feedback (ZA), the meridional advective effect (VA), the Ekman pumping feedback (EK), the mean current effect (MA) and the thermocline feedback (TH) and the nonlinear

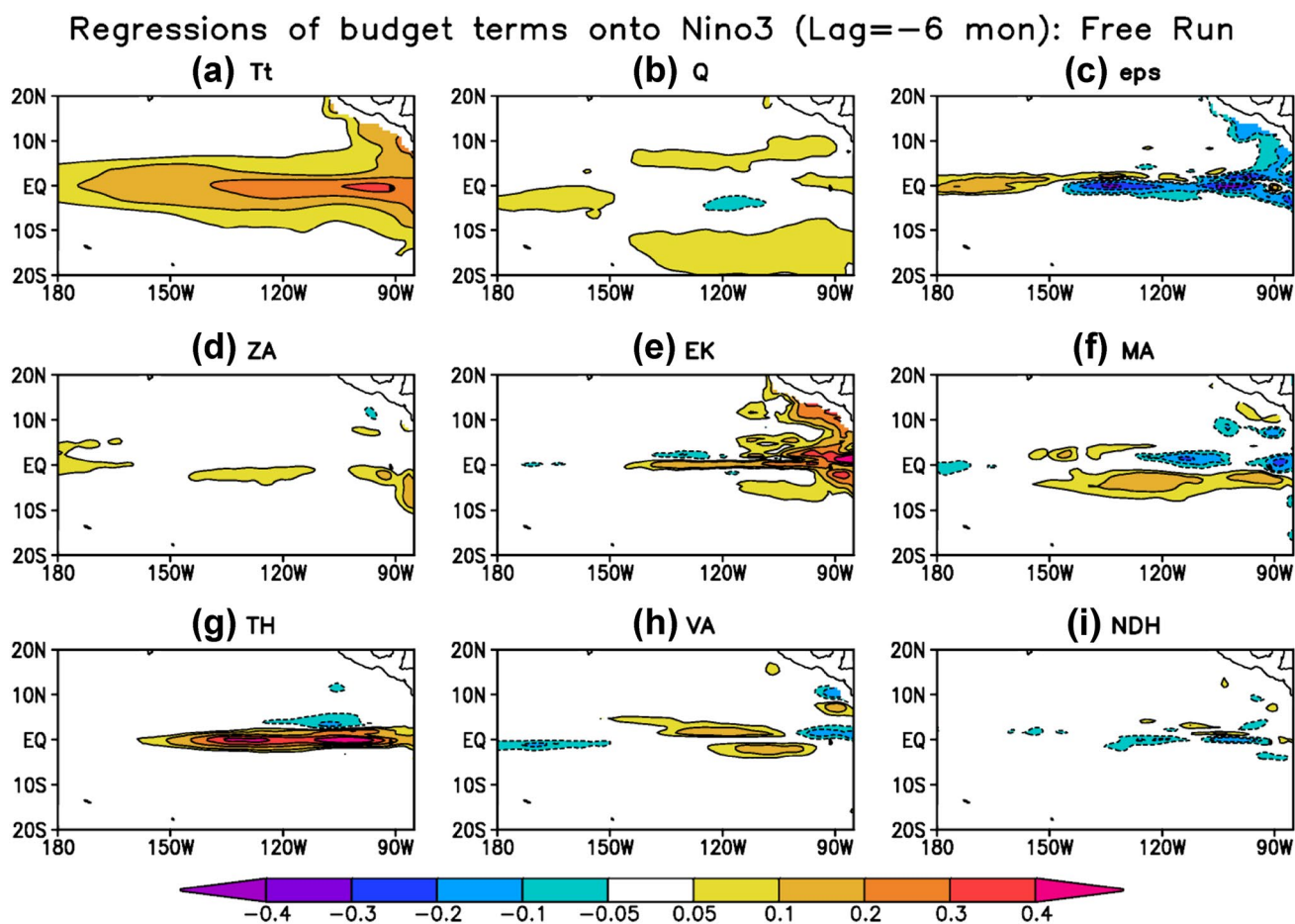


Fig. 9 Same as in Fig. 8, but in the Free Run

dynamical heating (NDH). Compared with the Bjerknes index (Jin et al. 2006; Kim and Jin 2011), the ENSO diagnostics with Eq. (3) has the advantage of applying fewer assumptions and the inclusion of the nonlinear process (i.e., the NDH term) as well. Studies have suggested that the different feedback processes play different roles in ENSO evolutions. Generally, the terms of ZA, EK, MA and TH are recognized as important factors for ENSO evolutions (e.g., Bjerknes 1969; Suarez and Schopf 1988; Battisti and Hirst 1989; Jin 1997; Kang et al. 2001; Picaut et al. 1996), and the VA term is usually thought negligible (Jin et al. 2006; Kim and Jin 2011). On the other hand, the NDH term is suggested to be important for the existence of ENSO asymmetry (Jin et al. 2003; An and Jin 2004; DiNezio and Deser 2014).

To explore the evolution of above terms associated with ENSO, the lead-lag regressions against the Niño-3 index are calculated as in Kang et al. (2001), and these regressions are compared between the Free Run and the Nudged Run. For a better inter-comparison, the same heat budget diagnostics and corresponding analyses are

also conducted for GODAS (Behringer and Xue 2004), which is used as a substitute of observations in spite of uncertainties in current ocean data analyses (e.g., Zhu et al. 2012). Figures 5, 6 and 7 present the time-longitude sections of the lead-lag regressions averaged between 5°S and 5°N. Note that the results are not very sensitive to the choice of the meridional domain from 2°S–2°N to 7°S–7°N.

The time tendency of mixed layer temperature (Fig. 5a, d, g) for both simulations and GODAS show little propagation along the equator, but the developing and decaying processes of ENSO in the CFSv2L Free Run seem to last slightly longer than in the Nudged Run. For the local surface heat flux (Fig. 5b, e, h), both runs and GODAS also have a similar evolution, i.e., almost out of phase with the Niño-3 SST anomaly, suggesting a damping role during the ENSO evolution. For the residue term (Fig. 5c, f, i), while both runs exhibit ill-organized structures, GODAS and the Nudged Run has clearly larger amplitude, which is because of additional contributions from the data corrections by 3-dimensional data assimilation or surface nudging.

Regressions of budget terms onto Nino3 (Lag=-6 mon): Nudged Run

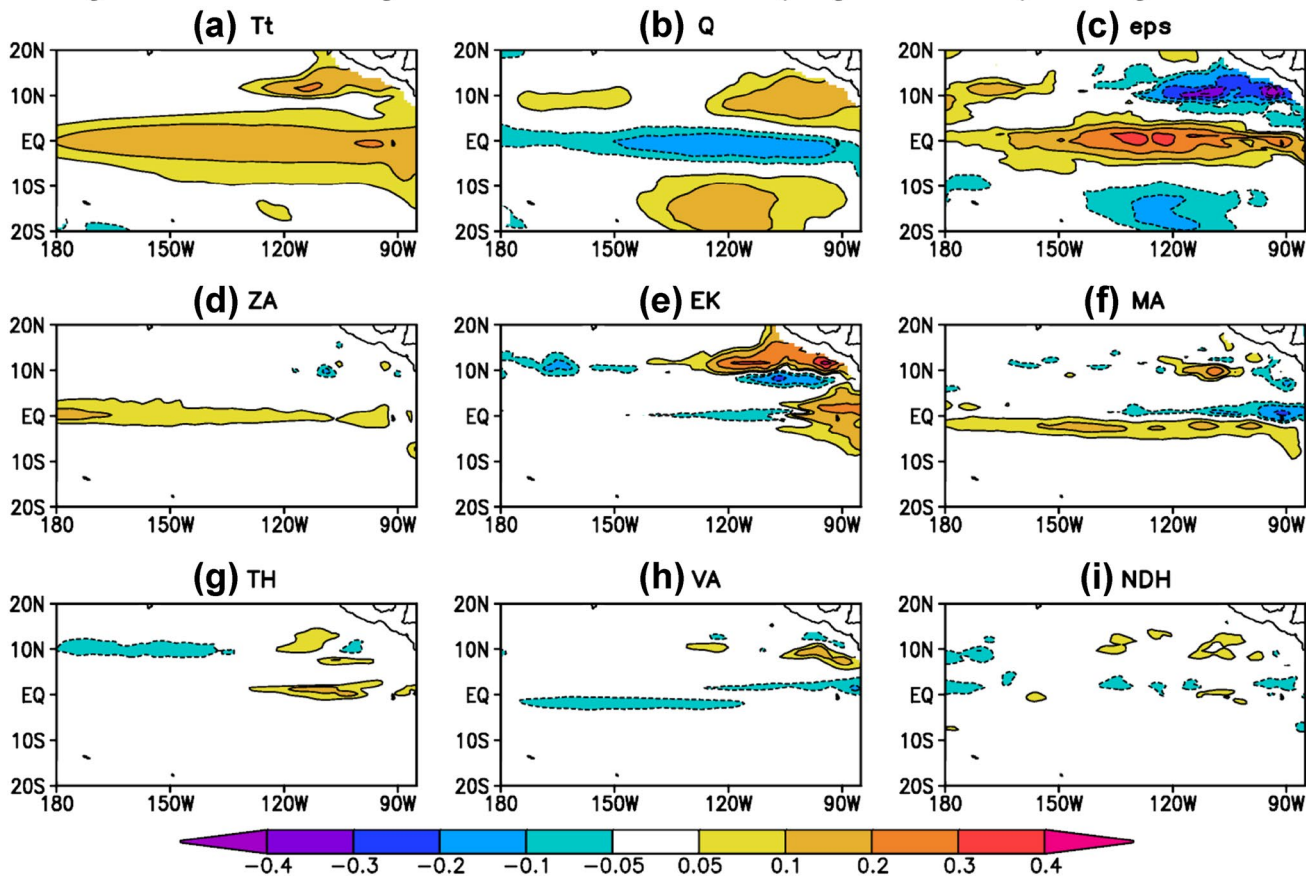


Fig. 10 Same as in Fig. 8, but in the Nudged Run

Figure 6 presents the regressions for terms about ZA, EK, MA and TH that were recognized as important factors for ENSO evolutions (e.g., Bjerknes 1969; Suarez and Schopf 1988; Battisti and Hirst 1989; Jin 1997; Kang et al. 2001; Picaut et al. 1996). For EK (Fig. 6b, f, j), whose effect during ENSO was first emphasized by Bjerknes (1969), GODAS and the Free and Nudged Runs show similar evolutions, i.e., it plays an important role during both the development (i.e., the negative lead times) and the decay (i.e., the positive lead times) stages of ENSO, but its effect is confined within the far eastern coastal region. For MA (Fig. 6c, g, k), GODAS and the Free and Nudged Runs also present similar lead-lag relationships with their Niño-3 index. Its decomposition suggests that the MA effect is dominated by the anomalous temperature advection by mean meridional current (i.e., $-\bar{v} \frac{\partial T'}{\partial y}$) (figures not shown).

Generally, the MA term varies in phase with ENSO, suggesting an amplifying role during the ENSO evolution. While this finding is consistent with many previous analyses like Battisti (1988) and Kang et al. (2001), it seems contrary to diagnostics with the Bjerknes index (e.g., Jin

et al. 2006; Kim and Jin 2011), possibly because the index applies many simplifications and assumptions.

For the ZA and TH terms, two most important feedbacks during ENSO evolutions (e.g., Suarez and Schopf 1988; Battisti and Hirst 1989; Jin 1997; Picaut et al. 1996), influences of surface nudging are seen more clearly. During the development phase of ENSO in GODAS and the Free Run, ZA (Fig. 6a, e) and TH (Fig. 6d, h) both have positive values, suggesting positive feedbacks during the growth phase of ENSO events. After its peak, negative values are present in ZA and TH (particularly in TH), which means they are contributing to the transition from the one phase of ENSO to the other. These roles played in the ENSO transitions actually is a reflection of the ocean memory, and are the basis for the ENSO predictability.

For the Nudged Run (Fig. 6i, l), the roles played by ZA and TH terms change considerably. Firstly, they become more in-phase with the Niño-3 index, which is particularly true for the thermocline feedback (i.e., TH). It means that the two feedbacks have more influence on amplitude than on phase transition of ENSO. Furthermore, the TH effect is more confined to the far eastern Pacific than that in the

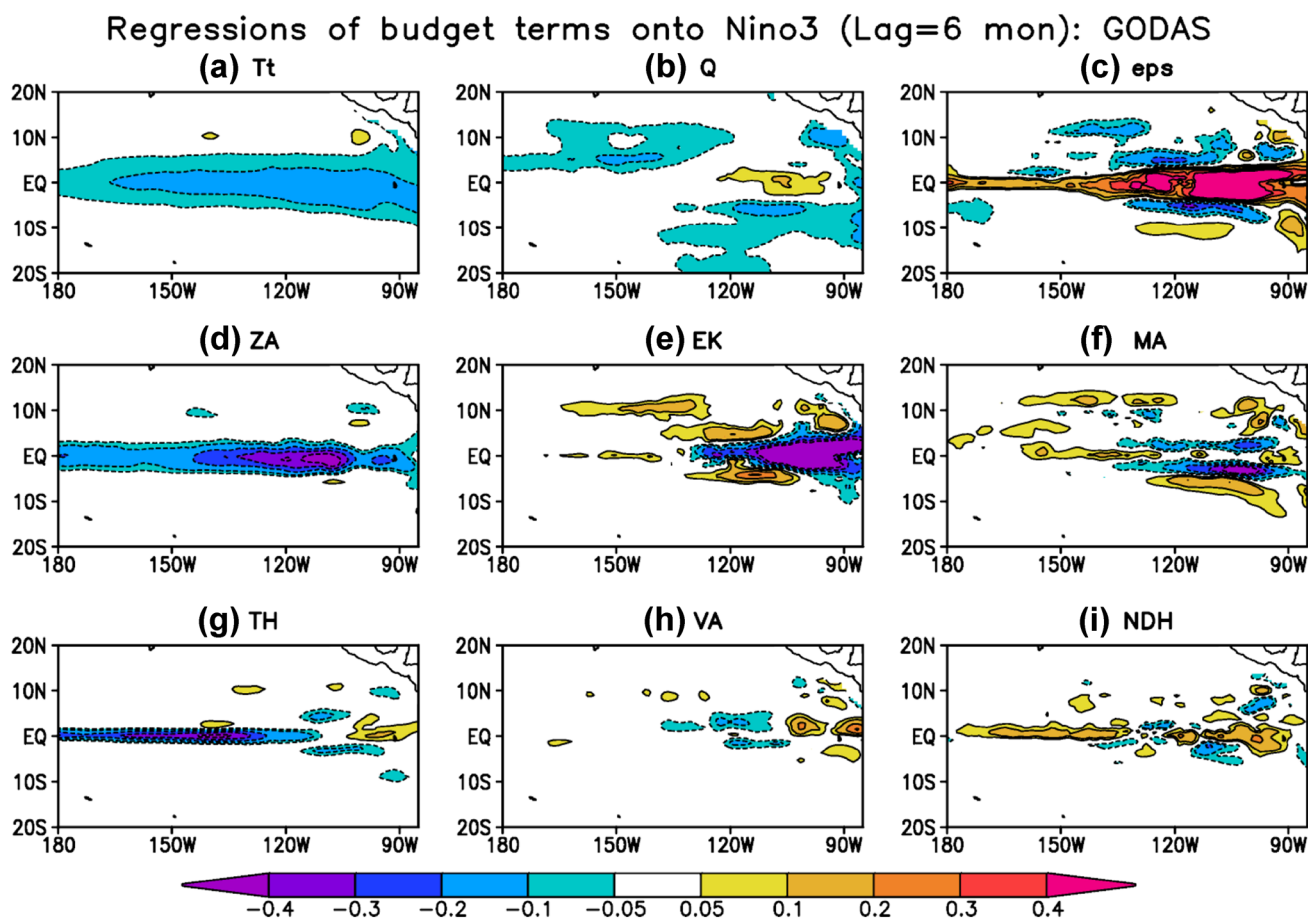


Fig. 11 Same as in Fig. 8, but at the lag time of 6 months (corresponding to 6 months after the peak phase of El Niño)

Free Run, and correspondingly has a weaker influence on the SST variability of the eastern Pacific. These results highlight that, although SST variations could be better represented by surface nudging, the physics behind might be modified and become unrealistic.

For the remaining two terms (i.e., VA and NDH; Fig. 7), they generally have much smaller values than others in GODAS and both runs. The finding supports assumptions made in previous studies (e.g., Jin et al. 2006; Kim and Jin 2011) which simply ignored them. However, they might be important for higher moments of ENSO which is not a focus of the present study; for example, Jin et al. (2003), An and Jin (2004) and DiNizeo and Deser (2014) suggested that NDH was important for the appearance of its non-zero skewness.

Horizontal distributions of the terms in Eq. (3) regressed onto Niño-3 index are shown in Figs. 8, 9 and 10 for the developing phase and in Figs. 11, 12 and 13 for the decaying phases of ENSO. During the developing phase (corresponding to the lag of -6 months in Figs. 5, 6, 7), significant differences between the Free Run and the Nudged Run appear in the TH term (Fig. 9g vs. Fig. 10g) and residue

term (Fig. 9c vs. Fig. 10c). Particularly, in the Free Run, the thermocline feedback (Fig. 9g) contributes the largest to the tendency of temperature anomalies (Fig. 9a) over the equatorial region, but the residue term (Fig. 9c) that includes the diffusive effects generally makes a negative contribution. The features are consistent with those in GODAS (Fig. 8). However, in the Nudged Run, the thermocline feedback (Fig. 10g) becomes much weaker, only contributing marginally to the tendency of temperature anomalies (Fig. 10a); in contrast, the residue term (Fig. 10c) becomes the most important contributor to the SST changes. A similar contrast between the Free and Nudged Runs is also present during the decay phase (corresponding to the lag of 6 months in Figs. 5, 6, 7) for the thermocline feedback (Fig. 12g vs. Fig. 13g) and the residue terms (Fig. 12c vs. Fig. 13c). The comparisons confirm again that surface nudging could significantly modify the physics that are responsible for the surface temperature evolution. Specifically, for CFSv2L, because of the surface nudging the tendency of temperature anomalies becomes unrealistically dominated by the residue term relative to other more physical terms like the thermocline feedback term.

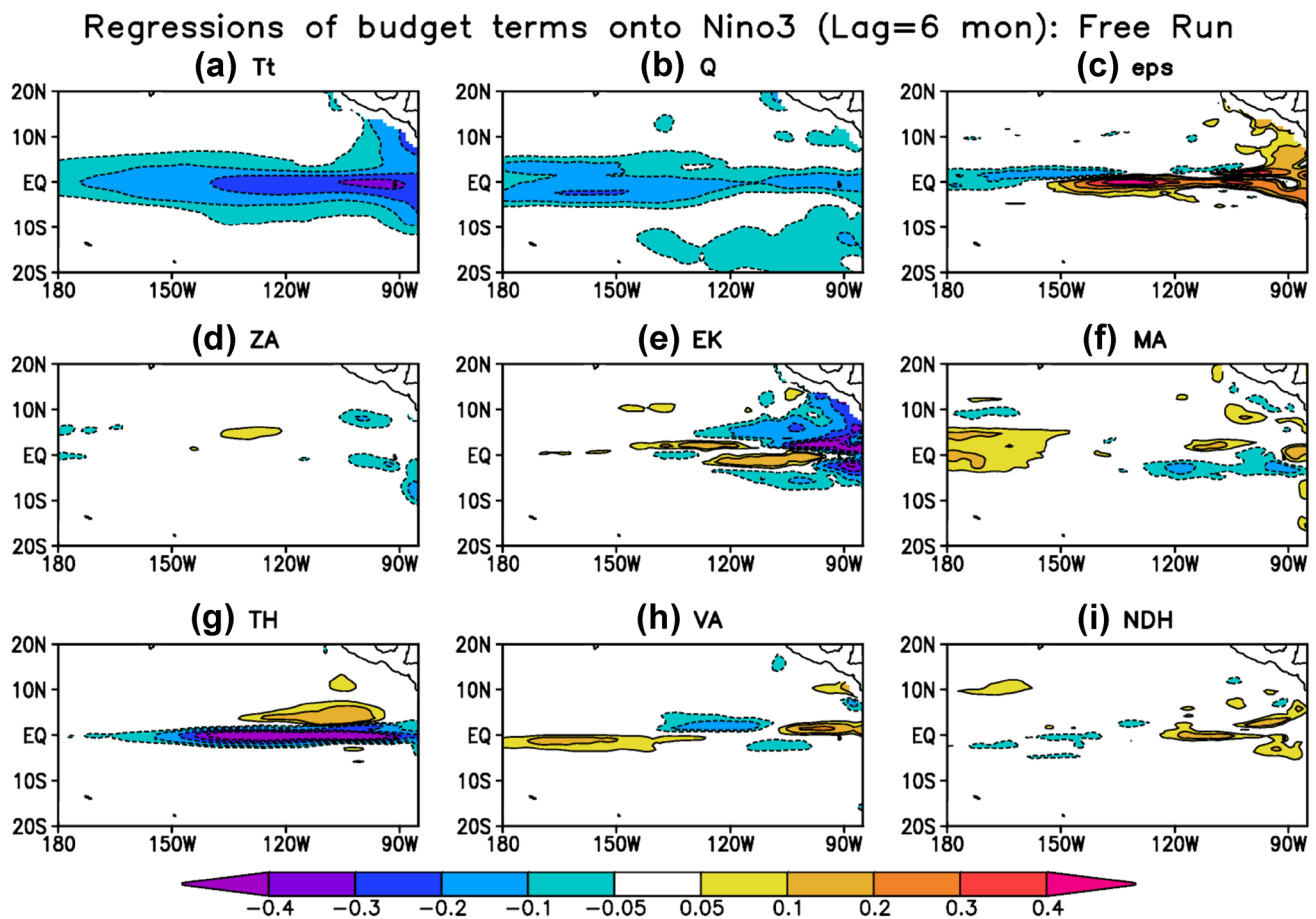


Fig. 12 Same as in Fig. 11, but in the Free Run

The weakened thermocline feedback associated with ENSO in the Nudged Run (Figs. 10g, 13 g) might be related to its weakened trade winds in the tropical Pacific (Fig. 3b). As shown above, the wind biases flatten the thermocline along the equator, and correspondingly the thermocline becomes unrealistically deep in the eastern Pacific in the Nudged Run (Fig. 4b), because of which the surface-thermocline connection becomes less efficient than in the Free Run or observations (Zelle et al. 2004; Zhu et al. 2015b), resulting in a weaker thermocline feedback.

4 Conclusion and discussion

Previous studies suggested that surface nudging could be used for many purposes. For example, because it can efficiently reconstruct the subsurface variability (e.g., Kumar et al. 2014a, b; Servonnat et al. 2015; Ray et al. 2015), it could be a useful method to initialize climate predictions (e.g., seasonal and decadal predictions; Keenlyside et al. 2005, 2008; Luo et al. 2005, 2007; Zhu et al. 2015a, 2017a; Swingedouw et al. 2013). Also, surface nudging

is the basis for climate models with flux adjustments. In this study, however, some problems associated with surface nudging are identified for climate simulations.

Specifically, two simulations based on a low-resolution version of the NCEP Climate Forecast System, version 2 (CFSv2L) were compared—one is free run and another one applies surface nudging. Firstly, it was found that, as expected, even though SST biases are removed, improvement in the simulations of climatological precipitation, surface winds and subsurface temperature (or the thermocline depth) are basin-dependent, which is exemplified by improvements in the tropical Atlantic, but degradations in the tropical Pacific. Further, based on a heat budget analysis of mixed layer temperature anomalies, the effect of surface nudging on coupled feedbacks was diagnosed. It was identified that surface nudging can significantly distort the dynamical feedbacks during ENSO. For example, while the thermocline feedback term played a critical role during the evolution of ENSO in CFSv2L, it only played a minor role in the nudged simulation. These results imply that, even though the simulation of surface

Regressions of budget terms onto Nino3 (Lag=6 mon): Nudged Run

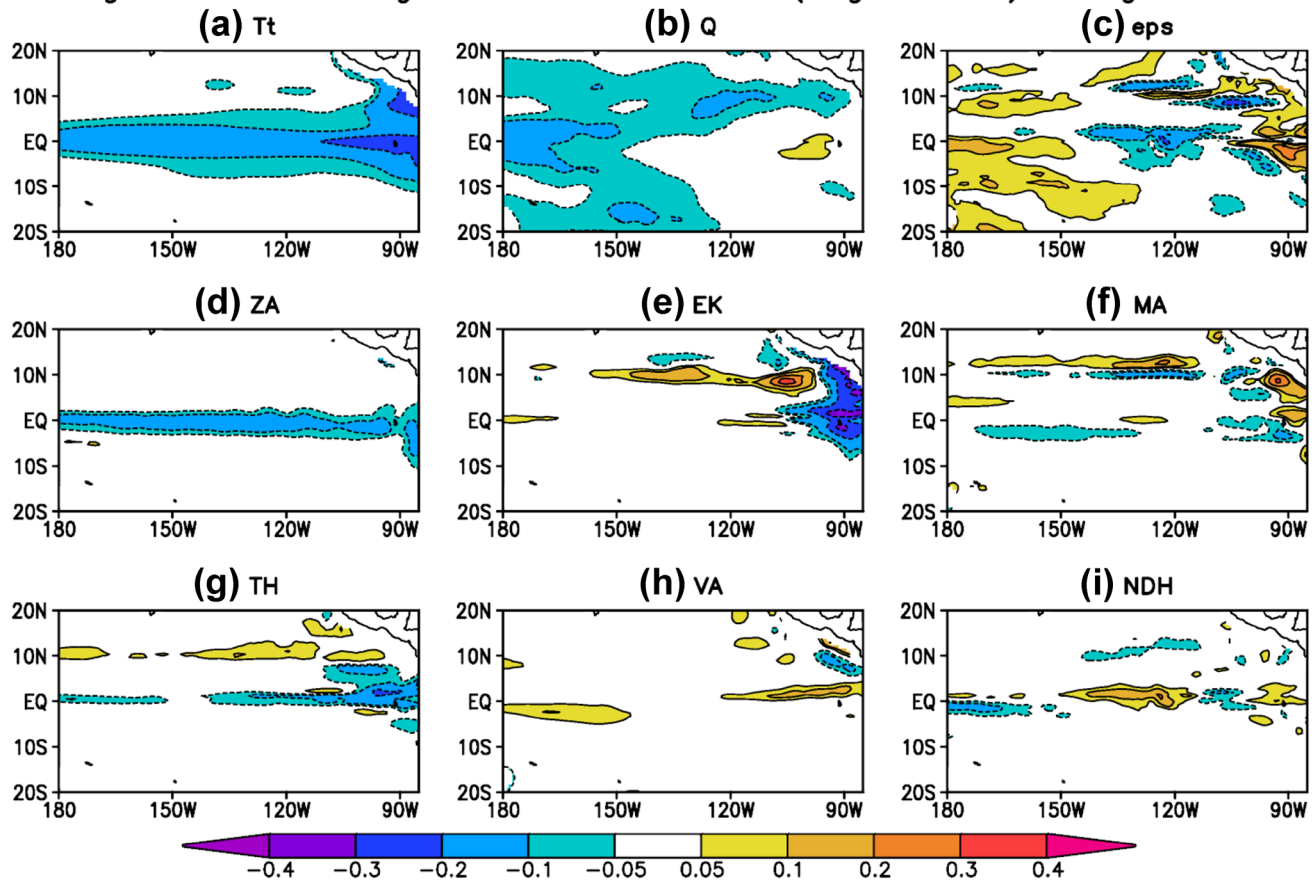


Fig. 13 Same as in Fig. 11, but in the Nudged Run

temperature could be improved in a climate model with surface nudging, the physics behind could be unrealistic.

It should be noted that the impact of surface nudging on model simulations is likely to highly depend on models. For example, while our study suggested that surface nudging degrades the simulation of zonal 10-m wind in CFSv2L (Fig. 3), an improvement was found by Magnusson et al. (2013a) in their model (i.e., the ECMWF IFS model, version 36r1). Also, in contrast to Xiang et al. (2012) who found that the thermocline feedback during ENSO was enhanced in their model by correcting the SST bias, our experiments suggest a weakened thermocline feedback by SST nudging. On the other hand, the performance of surface nudging could also depend on different basins. In terms of CFSv2L, it degrades the climatological simulations over the tropical Pacific, but it seems to improve the tropical Atlantic simulations.

The reason why the influence of surface nudging is basin- and model-dependent is likely to depend on various aspects. They are likely related to biases in the nudged simulation (or equivalently, the AMIP simulations with specified SSTs) and how these biases influence a free run

via air-sea interactions at the beginning of integration. For example, a large precipitation biases over an ocean basin will result in a reduced surface shortwave insolation. In a free run, a reduced surface shortwave insolation will result in a cooler mixed layer ocean temperature, and if the initial influence was to persist, will eventually result in cooler SST climatology and a reduction in precipitation. This scenario was likely responsible for differences in SST and precipitation in the Free and Nudged simulation over the Indian Ocean. In contrast, if the surface wind stress biases in the Nudged run were to dominate initially, a pathway to biases in the Free simulation would differ. Investigating these aspects in two simulations discussed here will be of interest, particularly in the context of the onset of model biases, and will be focus of a future analysis.

In addition to problems identified in this study, a previous study (Luo et al. 2011) also found another drawback in the SST-nudged simulation, that is, a spurious long-term trend in its generated ocean subsurface temperature. In particular, in their model a strong spurious cooling drift of the ocean subsurface temperature was identified (Luo et al. 2011), and they attributed it to large negative surface heat

flux damping when the model SSTs are strongly restored toward the observed values. They further suggested that the drawback could affect climate prediction skill.

Acknowledgements We thank NOAA's Climate Program Office, Climate Observation Division for their support.

References

- An S-I, Jin F-F (2004) Nonlinearity and asymmetry of ENSO. *J Clim* 17:2399–2412
- Balmaseda M, Mogensen K, Weaver A (2013) Evaluation of the ECMWF ocean reanalysis ORAS4. *Quart J R Meteor Soc* 139:1132–1161
- Battisti DS (1988) The dynamics and thermodynamics of a warming event in a coupled tropical atmosphere/ocean model. *J Atmos Sci* 45:2889–2919
- Battisti DS, Hirst AC (1989) Interannual variability in the tropical atmosphere–ocean model: influence of the basic state, ocean geometry and nonlinearity. *J Atmos Sci* 45:1687–1712
- Behringer DW, Xue Y (2004) Evaluation of the global ocean data assimilation system at NCEP: the Pacific Ocean. Eighth symposium on integrated observing and assimilation systems for atmosphere, oceans, and land surface, AMS 84th Annual Meeting, Washington State Convention and Trade Center, Seattle, Washington, pp 11–15
- Bjerknes J (1969) Atmospheric teleconnections from the equatorial Pacific. *Mon Weather Rev* 97:163–172
- DiNezio PN, Deser C (2014) Nonlinear controls on the persistence of La Niña. *J Clim* 27:7335–7355. doi:10.1175/JCLI-D-14-00033.1
- Huang B, Shukla J (1997) Characteristics of the interannual and decadal variability in a general circulation model of the tropical Atlantic Ocean. *J Phys Oceanogr* 27:1693–1712
- Jin F-F (1997) An equatorial ocean recharge paradigm for ENSO. Part I: conceptual model. *J Atmos Sci* 54:811–829
- Jin EK, Coauthors (2008) Current status of ENSO prediction skill in coupled ocean–atmosphere models. *Clim Dyn* 31:647–664
- Jin F-F, An S-I, Timmermann A, Zhao J (2003) Strong El Niño events and nonlinear dynamical heating. *Geophys Res Lett* 30(3):1120. doi:10.1029/2002GL016356
- Jin F-F, Kim ST, Bejarano L (2006) A coupled-stability index for ENSO. *Geophys Res Lett* 33:L23708. doi:10.1029/2006GL027221
- Kang I-S, An S-I, Jin FF (2001) A systematic approximation of the SST anomaly equation for ENSO. *J Meteor Soc Jpn* 79:1–10
- Keenlyside NS, Latif M, Botzet M, Jungclaus J, Schulzweida U (2005) A coupled method for initializing El Niño–Southern Oscillation forecasts using sea surface temperature. *Tellus* 57A:340–356
- Keenlyside NS, Latif M, Jungclaus J, Kornbluh L, Roeckner E (2008) Advancing decadal-scale climate prediction in the North Atlantic sector. *Nature* 453:84–88
- Kim ST, Jin F-F (2011) An ENSO stability analysis. Part I: results from a hybrid coupled model. *Clim Dyn* 36:1593–1607. doi:10.1007/s00382-010-0796-0
- Kohyama T, Tozuka T (2016) Seasonal variability of the relationship between SST and OLR in the Indian Ocean and its implications for initialization in a CGCM with SST nudging. *J Oceanogr* 72:327–337
- Kröger J, Kucharski F (2011) Sensitivity of ENSO characteristics to a new interactive flux correction scheme in a coupled GCM. *Clim Dyn* 37:119–137
- Kumar A, Wang H, Xue Y, Wang W (2014a) How much of monthly subsurface temperature variability in the equatorial Pacific can be recovered by the specification of sea surface temperatures? *J Clim* 27:1559–1577
- Kumar A, Jha B, Wang H (2014b) Attribution of SST variability in global oceans and the role of ENSO. *Clim Dyn* 43:209–220. doi:10.1007/s00382-013-1865-y
- Luo J-J, Masson S, Behera S, Shingu S, Yamagata T (2005) Seasonal climate predictability in a coupled OAGCM using a different approach for ensemble forecasts. *J Clim* 18:4474–4497
- Luo J-J, Masson S, Behera SK, Yamagata T (2007) Experimental forecasts of the Indian Ocean dipole using a coupled OAGCM. *J Clim* 20:2178–2190
- Luo J-J, Behera S, Masumoto Y, Yamagata T (2011) Impact of global ocean surface warming on seasonal-to-interannual climate prediction. *J Clim* 24:1626–1646. doi:10.1175/2010JCLI3645.1
- Magnusson L, Balmaseda MA, Molteni F (2013a) On the dependence of ENSO simulation on the coupled model mean state. *Clim Dyn* 41:1509–1525
- Magnusson L, Balmaseda MA, Corti S, Molteni F, Stockdale T (2013b) Evaluation of forecast strategies for seasonal and decadal forecasts in presence of systematic model errors. *Clim Dyn* 41:2393–2409
- Manganello JV, Huang B (2009) The influence of systematic errors in the Southeast Pacific on ENSO variability and prediction in a coupled GCM. *Clim Dyn* 32:1015–1034
- Meehl GA, Coauthors (2014) Decadal climate prediction: an update from the trenches. *Bull Am Meteor Soc* 95:243–267
- Moura AD, Shukla J (1981) On the dynamics of the droughts in north-east Brazil: observations, theory and numerical experiments with a general circulation model. *J Atmos Sci* 38:2653–2675
- Pan X, Huang B, Shukla J (2011) The influence of mean climate on the equatorial Pacific seasonal cycle and ENSO: simulation and prediction experiments using CCSM3. *Clim Dyn* 37:325–341. doi:10.1007/s00382-010-0923-y
- Picaut J, Ioualalen M, Menkes C, Delcroix T, McPhaden M (1996) Mechanism of the zonal displacements of the Pacific warm pool, implications for ENSO. *Science* 274:1486–1489
- Ray S, Swingedouw D, Mignot J, Guilyardi E (2015) Effect of surface restoring on subsurface variability in a climate model during 1949–2005. *Clim Dyn* 44:2333–2349
- Reynolds RW, Rayner NA, Smith TM, Stokes DC, Wang W (2002) An improved in situ and satellite SST analysis for climate. *J Clim* 15:1609–1625
- Saha S, Coauthors (2010) The NCEP climate forecast system reanalysis. *Bull Am Meteor Soc* 91:1015–1057
- Saha S, Coauthors (2014) The NCEP climate forecast system version 2. *J Clim* 27:2185–2208
- Sausen R, Barthel K, Hasselmann K (1988) Coupled ocean–atmosphere models with flux correction. *Clim Dyn* 2:145–163
- Servonnat J, Mignot J, Guilyardi E, Swingedouw D, Séférian R, Labetoulle S (2015) Reconstructing the subsurface ocean decadal variability using surface nudging in a perfect model framework. *Clim Dyn* 44:315–338. doi:10.1007/s00382-014-2184-7
- Spencer H, Sutton R, Slingo JM (2007) El Niño in a coupled climate model: sensitivity to changes in mean state induced by heat flux and wind stress corrections. *J Clim* 20:2273–2298
- Suarez MJ, Schopf PS (1988) A delayed action oscillator for ENSO. *J Atmos Sci* 45:3283–3287
- Swingedouw D, Mignot J, Labetoulle S, Guilyardi E, Madec G (2013) Initialisation and predictability of the AMOC over the last 50 years in a climate model. *Clim Dyn* 40:2381–2399
- Vecchi GA et al (2014) On the seasonal forecasting of regional tropical cyclone activity. *J Clim* 27:7994–8016. doi:10.1175/JCLI-D-14-00158.1

- Wang H, Kumar A, Wang W (2013) Characteristics of subsurface ocean response to ENSO assessed from simulations with the NCEP Climate Forecast System. *J Clim* 26:8065–8083
- Xiang B, Wang B, Ding Q, Jin F, Fu X, Kim HJ (2012) Reduction of the thermocline feedback associated with mean sst bias in ENSO simulation. *Clim Dyn* 39:1413–1430
- Xie P, Arkin P (1997) Global precipitation: a 17-year monthly analysis based on gauge observations, satellite estimates, and numerical model outputs. *Bull Am Meteor Soc* 78:2539–2558
- Xue Y, Chen M, Kumar A, Hu Z-Z, Wang W (2013) Prediction skill and bias of tropical Pacific sea surface temperatures in the NCEP Climate Forecast System version 2. *J Clim* 26:5358–5378
- Zelle H, Appeldoorn G, Burgers G, van Oldenborgh GJ (2004) The relationship between sea surface temperature and thermocline depth in the eastern equatorial Pacific. *J Phys Oceanogr* 34:643–655. doi:[10.1175/2523.1](https://doi.org/10.1175/2523.1)
- Zhu J, Shukla J (2013) The role of air-sea coupling in seasonal prediction of Asian-Pacific summer monsoon rainfall. *J Clim* 26:5689–5697. doi:[10.1175/JCLI-D-13-00190.1](https://doi.org/10.1175/JCLI-D-13-00190.1)
- Zhu J, Zhou G-Q, Zhang R-H, Sun Z (2011) On the role of oceanic entrainment temperature (T_e) in decadal changes of El Niño/Southern Oscillation. *Ann Geophys* 29:529–540. doi:[10.5194/angeo-29-529-2011](https://doi.org/10.5194/angeo-29-529-2011)
- Zhu J, Huang B, Balmaseda MA (2012) An ensemble estimation of the variability of upper-ocean heat content over the tropical Atlantic Ocean with multi-ocean reanalysis products. *Clim Dyn* 39:1001–1020. doi:[10.1007/s00382-011-1189-8](https://doi.org/10.1007/s00382-011-1189-8)
- Zhu J, Kumar A, Wang H, Huang B (2015a) Sea surface temperature predictions in NCEP CFSv2 using a simple ocean initialization scheme. *Mon Weather Rev* 143:3176–3191
- Zhu J, Kumar A, Huang B (2015b) The relationship between thermocline depth and SST anomalies in the eastern equatorial Pacific: seasonality and decadal variations. *Geophys Res Lett* 42:4507–4515. doi:[10.1002/2015GL064220](https://doi.org/10.1002/2015GL064220)
- Zhu J, Kumar A, Lee H-C, Wang H (2017a) Seasonal predictions using a simple ocean initialization scheme. *Clim Dyn*. doi:[10.1007/s00382-017-3556-6](https://doi.org/10.1007/s00382-017-3556-6)(published online)
- Zhu J, Wang W, Kumar A (2017b) Simulations of MJO propagation across the Maritime continent: impacts of SST feedback. *J Clim* 30:1689–1704. doi:[10.1175/JCLI-D-16-0367.1](https://doi.org/10.1175/JCLI-D-16-0367.1)